Aerobiologia (2012) 28:1–11
DOI 10.1007/s10453-011-9206-2

ORIGINAL PAPER

Isolates of *Fusarium graminearum* collected 40–320 meters above ground level cause Fusarium head blight in wheat and produce trichothecene mycotoxins

D. G. Schmale III · S. D. Ross · T. L. Fetters · P. Tallapragada · A. K. Wood-Jones · B. Dingus

Received: 29 November 2010 / Accepted: 2 April 2011 / Published online: 20 April 2011

Abstract The aerobiology of fungi in the genus *Fusarium* is poorly understood. Many species of *Fusarium* are important pathogens of plants and animals and some produce dangerous secondary metabolites known as mycotoxins. In 2006 and 2007, autonomous unmanned aerial vehicles (UAVs) were used to collect *Fusarium* 40–320 m above the ground at the Kentland Farm in Blacksburg, Virginia. Eleven single-spored isolates of *Fusarium graminearum* (sexual stage *Gibberella zeae*) collected with autonomous UAVs during fall, winter, spring, and summer months caused Fusarium head blight on a susceptible cultivar of spring wheat. Trichothecene genotypes were determined for all 11 of the isolates; nine isolates were DON/15ADON, one isolate was DON/3ADON, and one isolate was NIV. All of the isolates produced trichothecene mycotoxins *in planta* consistent with their trichothecene genotypes. To our knowledge, this is the first report of a NIV isolate of *F. graminearum* in Virginia, and DON/3ADON genotypes are rare in populations of the fungus recovered from infected wheat plants in the eastern United States. Our data are considered in the context of a new aerobiological framework based on atmospheric transport barriers, which are Lagrangian coherent structures present in the mesoscale atmospheric flow. This framework aims to improve our understanding of population shifts of *F. graminearum* and develop new paradigms that may link field and atmospheric populations of toxigenic *Fusarium* spp. in the future.

Keywords Fungi · Pathogen · Aerosol · Wheat · Barley · Unmanned aerial vehicles · Bio-threat · Atmospheric modeling · Long-distance transport · Mycotoxin · Atmospheric transport barrier

D. G. Schmale III (✉) · T. L. Fetters · B. Dingus
Department of Plant Pathology, Physiology and Weed Science, Virginia Tech, Blacksburg, VA 24061, USA
e-mail: dschmale@vt.edu

S. D. Ross · P. Tallapragada
Department of Engineering Science and Mechanics, Virginia Tech, Blacksburg, VA 24061, USA

A. K. Wood-Jones
Department of Entomology and Plant Pathology, Mississippi State University, Mississippi State, MS 39762, USA

1 Introduction

Fusarium is one of the most important genera of fungi in the world. The genus contains at least 80 biological species (Leslie and Summerell 2006), with 100 or more proposed phylogenetic species. Some *Fusarium* spp. cause rots (Wang and Jeffers 2000), cankers (Schmale and Gordon 2003), blights (Schmale and Bergstrom 2003), and wilts (Chaimovitsh et al. 2006) of important agricultural crops. Others are saprophytes, colonizing dead and decaying

organic matter in a variety of ecosystems (Dill-Macky and Jones 2000). Some *Fusarium* spp. produce dangerous mycotoxins, posing a serious threat to the health of humans and livestock (McMullen et al. 1997; Ichinoe et al. 1983; Bush et al. 2004).

Many *Fusarium* spp. are well suited for atmospheric dispersal. *Fusarium equiseti* (Corda) Saccardo, a common soil inhabitant worldwide, produces whip-like macroconidia (approximately 100 μm in length) that may be picked up from cushion-shaped spore masses called sporodochia and transported away from the ground in turbulent air currents (Fernando et al. 2000). *Fusarium oxysporum* Schlechtendahl emend. Synder and Hansen, a common wilt pathogen of many agricultural crops, produces copious amounts of kidney-shaped microconidia (approximately 10 μm in length) that may be easily dislodged from conidiophores for transport through the atmosphere (Katan et al. 1997). *Fusarium graminearum* Schwabe, causal agent of Fusarium head blight (FHB) of wheat and barley, has a perfect state (*Gibberella zeae*) that produces flask-shaped "spore guns" called perithecia that forcibly discharge ascospores (approximately 30 μm in length) into the air (Schmale et al. 2005). These spores may be transported over long distances through the atmosphere to susceptible wheat and barley crops during the growing season (Francl et al. 1999; Maldonado-Ramirez et al. 2005).

Fusarium graminearum is arguably one of the most important members of the genus. Wheat and barley grain infected with *F. graminearum* are often contaminated with the trichothecene mycotoxins deoxynivalenol (DON) and nivalenol (NIV) (Goswami and Kistler 2005). In the 1990s, FHB and resulting mycotoxin contamination contributed to over $4 billion in losses in the United States and Canada (McMullen et al. 1997). Isolates of *F. graminearum* that produce DON may also produce acetylated derivatives of DON (e.g., 3-acetyl-DON (3ADON) and 15-acetyl-DON (15ADON)). Recent studies suggest that field populations of *F. graminearum* in the United States are changing, and these changes might be attributed in part to the types of mycotoxins (DON/15ADON, DON/3ADON, or NIV) that are being produced by the fungus (Gale et al. 2007; Guo et al. 2008; Ward et al. 2008). Such large-scale changes in the structure of *F. graminearum* field populations might be coupled with punctuated episodes of long-distance transport of pathogen spores (Maldonado-Ramirez et al. 2005; Schmale et al. 2006), but little is known about the origin, aggressiveness, and mycotoxin production of atmospheric populations of *F. graminearum*. Despite over two decades of research on FHB, we have yet to develop a complete aerobiological framework for *F. graminearum*.

Natural environmental and biological fluid flows, such as those found in the atmosphere, oceans, and cardiovascular flow, exhibit complex dynamics (Isard and Gage 2001; Aylor 2003; Bowman et al. 2007; d'Ovidio et al. 2004; Shadden and Taylor 2008). This complexity is actually a boon for the transport of mobile passive agents (Inanc et al. 2005; Senatore and Ross 2008). Despite the flow complexity, it is possible to discern the transport network of dynamical structures that geometrically organize the motion over scales of interest (Lekien and Ross 2010; Senatore and Ross 2011), and some biological species are already known to track structures related to transport in the geophysical environment (Tew Kai et al. 2009). In the context of long-range atmospheric transport of *Fusarium*, atmospheric transport barriers (ATBs) that separate air masses could play a significant role in the movement of spores among habitats. These structures can be predicted and tracked, based on forecast models and observations, using dynamical systems methods and concepts such as Lagrangian coherent structures, invariant manifolds, and almost-invariant sets (Lekien et al. 2005; Dellnitz et al. 2005; Froyland et al. 2007; Froyland and Padberg 2009; Stremler et al. 2011).

In the present study, we test the ability of 11 isolates of *F. graminearum* collected with autonomous UAVs to cause disease in wheat and produce mycotoxins. These isolates were collected 40–320 m above ground level (AGL) during fall, winter, spring, and summer months in 2006 and 2007. The concept of moving ATBs is used to provide a framework for understanding the long-distance transport of *F. graminearum* in the context of airborne biological invasions. The specific objectives of this study were to (1) examine the ability of 11 isolates of *F. graminearum* collected with UAVs to cause FHB on a susceptible cultivar of wheat and produce mycotoxins and (2) develop and test a geometric framework based on ATBs for understanding the long-distance transport of *F. graminearum*. An abstract on a portion of this work has been published (Schmale et al. 2010).

2 Materials and methods

Field studies were conducted at Virginia Tech's Kentland Farm in Blacksburg, VA in 2006 and 2007. The Kentland Farm consists of nearly 2,000 acres of agricultural fields.

2.1 Autonomous unmanned aerial vehicles (UAVs)

Autonomous (self-controlling) UAVs were used to collect *Fusarium*. The UAV platform was a Senior Telemaster equipped with remote-controlled microbe-sampling devices, a MicroPilot 2028g autopilot computer, and suite of telemetry sensors as described by Schmale et al. (2008) (Fig. 1, left). The UAVs were programmed to fly a circular sampling pattern of an approximate radius of 100 m around a single GPS waypoint (N37.1971, W 80.57375) at 60 km/h at a series of preset altitudes (Table 1). Each UAV was configured with an RxMux (Dingus et al. 2007) to allow the ground-based pilots to have real-time dynamic control of the UAV. The microbe-sampling devices consisted of four vertically mounted Petri plates (Fig. 1, left). Each plate contained a *Fusarium* selective medium as described by Schmale et al. (2006). The sampling devices were closed during takeoff and landing and were opened during autonomous flight for durations of 10–15 min. Immediately following each sampling mission, the exposed plates were removed from the UAVs and stored in small plastic containers for transport to the laboratory.

2.2 Collection and culturing of *Fusarium*

Collection plates from UAV sampling missions contained a *Fusarium* selective medium as described by Schmale et al. (2006). Plates were incubated in the laboratory at ambient room temperature for 5–7 days to allow white, fuzzy colonies of *Fusarium* to develop (Fig. 1, right). Each tentative *Fusarium* colony was transferred to plates of one-fourth-strength potato dextrose agar (PDA) using a sterile wooden toothpick. Pure cultures of *Fusarium* were established by transferring a single asexual spore (macroconidium) from each culture onto one-fourth-strength PDA, and these pure isolates were grown in potato dextrose broth for 4 days on a rotating shaker at 150 rpm. The resulting mycelium was lyophilized for 24 h, and DNA was extracted from homogenized mycelium using Qiagen's DNeasy Plant Mini Kit (Qiagen, Inc. USA, Valencia, CA) following the manufacturer's protocols.

2.3 Identification of *F. graminearum* and trichothecene genotyping

A portion of the translation elongation factor (TEF) gene (Geiser et al. 2004) was PCR amplified and sequenced from each of the 11 isolates tentatively identified as *F. graminearum* based on culture characteristics (shape and size of macroconidia, absence of microconidia) and colony morphology (red pigment on PDA) as described in Leslie and Summerell (2006). SeqMan Pro (Lasergene v8.1.1, Madison, WI) was used to trim and align sequences. BLAST queries were performed against a curated TEF database for *Fusarium* and against GenBank. Trichothecene genotyping was conducted as described in Schmale et al. (2011). Briefly, two multiplex PCR assays were used to evaluate trichothecene genotypes (Ward et al. 2002). These assays relied on the amplification of portions of two genes, *TRI3* and *TRI12*, that provide an indication of mycotoxin production in *F. graminearum* (Ward et al. 2002). Only one trichothecene genotype-specific amplicon is produced for each of the two genes.

2.4 Inoculations and disease assessments

The susceptible spring wheat cultivar Norm was used for all of the inoculations. Plants were grown in a growth chamber under controlled environmental conditions. Replicated pots were planted with five wheat seeds, and three spikes on primary tillers from three separate plants were selected for inoculations. Inoculations with individual isolates were confined to separate pots. All inoculations were performed at anthesis, when approximately half of the spikes in the growth chamber were extruding anthers. Three spikes were inoculated for each of the 11 isolates (Table 1, A–K). Autoclaved tips of round toothpicks (approximately 5–6 mm long) were rolled across sporulating culture plates of each of the isolates (one-fourth PDA, 10 days old). The tips of six spikelets (two at the top, two at the middle, and two at the bottom of the spike) were cut with sterile scissors, and a single toothpick-tip laden with fungus was inserted into each cut spikelet with sterile forceps. Wounded, non-inoculated plants served as controls. Three inoculated and three control

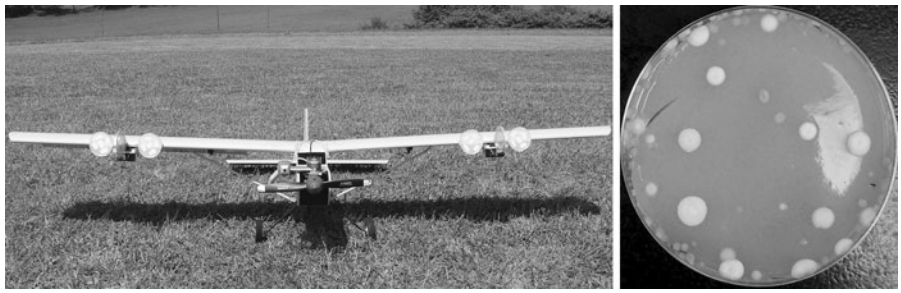

Fig. 1 An autonomous unmanned aerial vehicle (UAV) equipped with remote-operated sampling devices to collect *Fusarium* in the lower atmosphere (*left*). The sampling devices are closed during takeoff and landing and opened once the UAV is aloft at its target sampling altitude. White colonies of *Fusarium* are recovered from collection plates containing *Fusarium* selective medium after an incubation period of 5–7 days in the laboratory (*right*)

spikes were harvested at 14 days. The number of spikelets showing symptoms of FHB (premature bleaching) was recorded for each of the spikes, and this number was divided by the total number of spikelets to give a measure of FHB severity. Following disease assessments, individual spikes were placed in 15-mL sterile conical vials and stored at −20°C for downstream mycotoxin analyses.

2.5 Determination of trichothecene mycotoxins

Trichothecene mycotoxins were determined from wheat spikes harvested at 14 days using an Agilent 6890/5975 GC/MS operating in selected ion monitoring (SIM) mode. The following target and reference ions were used for each of the mycotoxins: DON, 422.2, 497.3, and 512.2; 3ADON/15ADON, 392.20, 467.10; and NIV, 289.10, 482.3, 510.3. The initial column temperature was held at 150°C for 1 min and increased to 280 C at a rate of 30°C/min and held constant for 5 min. The injection temperature was set at 300°C, and the flow rate of the column was 1 ml/min. DON, 3ADON, 15ADON, and NIV were quantified in the samples based on retention times and profiles of resulting ions using a linear regression model based on pure trichothecene standards (Biopure, Austria) at concentrations of 0.1, 0.5, 1.0, 5.0, and 10.0 ppm.

Spikes were removed from −20°C storage and dried in a 50°C incubator for 24 h. A bead-beating protocol as described by Reaver and Schmale (2007) was used to homogenize the wheat spikes. Briefly, each individual wheat spike was cut into small portions and placed in 7-mL HDPE vials containing 13.7 mm chrome balls. Spikes were homogenized using a MiniBeadBeater-96 (BioSpec products, Bartlesville, OK) operating at 2,100 oscillations per minute for 25 s. Mycotoxins were extracted from 0.1 g of homogenized tissue in 1 mL of acetonitrile/water (86:14) on a shaker at 200 rpm for 1 h. The liquid fraction containing mycotoxins was then passed through an Alumina: C18 SPE column for clean-up. A 250 μL aliquot of the flow through was transferred to a glass test tube and evaporated to dryness using a nitrogen evaporator set at 55°C. Samples were first screened for trichothecene mycotoxins following an initial derivatization step using 50 μL of TMSI for 10 min, and 125 μL of isooctane was added to each tube followed by 125 μL of water. Samples were vortexed for 10 s, and 150 μL of the isooctane supernatant containing the mycotoxins was removed and transferred to chromatography vials for GC/MS analysis. Since many of the calculated values from the initial extraction were well outside the range of standards, the samples were evaporated and reconstituted in 400 μL of acetonitrile/water, derivatized a second time using TMSI/TMCS (100:1), and resuspended in 250 μL isooctane (a final dilution factor of 10). This process allowed us to produce responses within the range of our standard curve (i.e., so no sample responses were greater than 10.0 ppm following the second dilution step).

2.6 Methods for ATB determination surrounding sampling intervals

ATBs were approximated using the method of Lagrangian coherent structures (LCSs). In the three-dimensional atmosphere, LCSs are time-evolving

Table 1 Isolates of *Fusarium graminearum* collected with unmanned aerial vehicles 40–320 m above ground level at Virginia Tech's Kentland Farm during fall, winter, spring, and summer months

Fusarium graminearum isolate ID	*Tri3/Tri12* genotype	Season	Date	Time (UTC)[a]	Colonies of *Fusarium*[b]	Mean altitude above ground level (m)[c]
A	DON/15ADON	Summer	September 16, 2006	20:30	19	97
B	DON/15ADON	Fall	October 08, 2006	15:30	9	99
C	DON/15ADON	Fall	November 10, 2006	21:55	8	100
D	DON/15ADON	Fall	November 11, 2006	18:20	8	100
E	DON/15ADON	Winter	December 18, 2006	18:00	4	100
F	DON/15ADON	Spring	May 01, 2007	14:00	36	100
G	NIV	Spring	May 01, 2007	15:00	21	100
H	DON/15ADON	Spring	May 09, 2007	20:00	10	100
I	DON/15ADON	Summer	July 02, 2007	19:00	13	40
J	DON/15ADON	Summer	July 02, 2007	19:00	6	120
K	DON/3ADON	Summer	July 03, 2007	16:10	6	324

Sequencing of a portion of the translation elongation factor (TEF) gene and PCR-based genotyping studies was conducted to identify the isolates to species and to classify them according to their trichothecene genotype, respectfully

[a] The start time of the sampling mission (plates open)

[b] Total number of colonies of *Fusarium* collected across four sampling plates

[c] Mean altitude above ground level as calculated from the data recorded onboard the UAV during the course of the sampling mission

two-dimensional surfaces that parse the atmospheric flow into qualitatively different, and highly mobile, air masses (Senatore and Ross 2011). The common technique to detect and compute LCSs is to calculate the largest finite time Lyapunov exponent (FTLE) field, a time-varying scalar field essentially measuring the stretching of air parcels in forward or backward time within the fluid domain (Haller and Yuan 2000). The underlying premise of the FTLE-LCS approach is that coherent structures in a flow are best represented by identifying and visualizing the surfaces of greatest trajectory separation. Ridges of the FTLE field are identified as the LCSs (Shadden et al. 2005). In the atmospheric context, we have repelling ATBs from forward-time FTLE and attracting ATBs from backward-time FTLE. We note that ATBs can be computed by other means, e.g., a transfer operator approach (Froyland et al. 2007), but given the ease of FTLE computations, the LCS-based approach was preferred.

To compute the forward and backward FTLE at a reference time t, a dense grid of particles was initialized at t covering the area of interest. In the present case, we used a grid of 400 × 400 particles initialized on the 900 hPa pressure surface, which approximates the height at which the samples were collected. An isobaric surface is used only for convenience (see, e.g., Lekien and Ross 2010), and the results are essentially identical if the parcels are initialized at nearby pressure surfaces, i.e., 875 hPa or 925 hPa (Tallapragada 2010). The virtual particles were numerically advected due to the time-varying wind using a standard-fourth-order Runga–Kutta numerical integration scheme. The time-varying wind data were provided by the large-scale assimilated meteorological products from the NOAA National Centers for Environmental Prediction (NCEP) North American Mesoscale (NAM) model. The data used consisted of North American grids of three-dimensional wind velocities with 12 km horizontal resolution, 26 standard pressure levels (vertical resolution), and 3 h temporal resolution. It is common practice (Tew Kai et al. 2009) to use a particle grid spacing which is much smaller (down to 10%) of the velocity grid. In our case, we used a particle grid spacing of 2 km, about 16.7% of the velocity grid spacing. At each reference time t, particles were advected forward and backward in time for 24 h to obtain particle trajectories. For times and locations between spatiotemporal grid points, cubic interpolation was used. Reference times were chosen to correspond to a 2-h time interval surrounding the sample containing

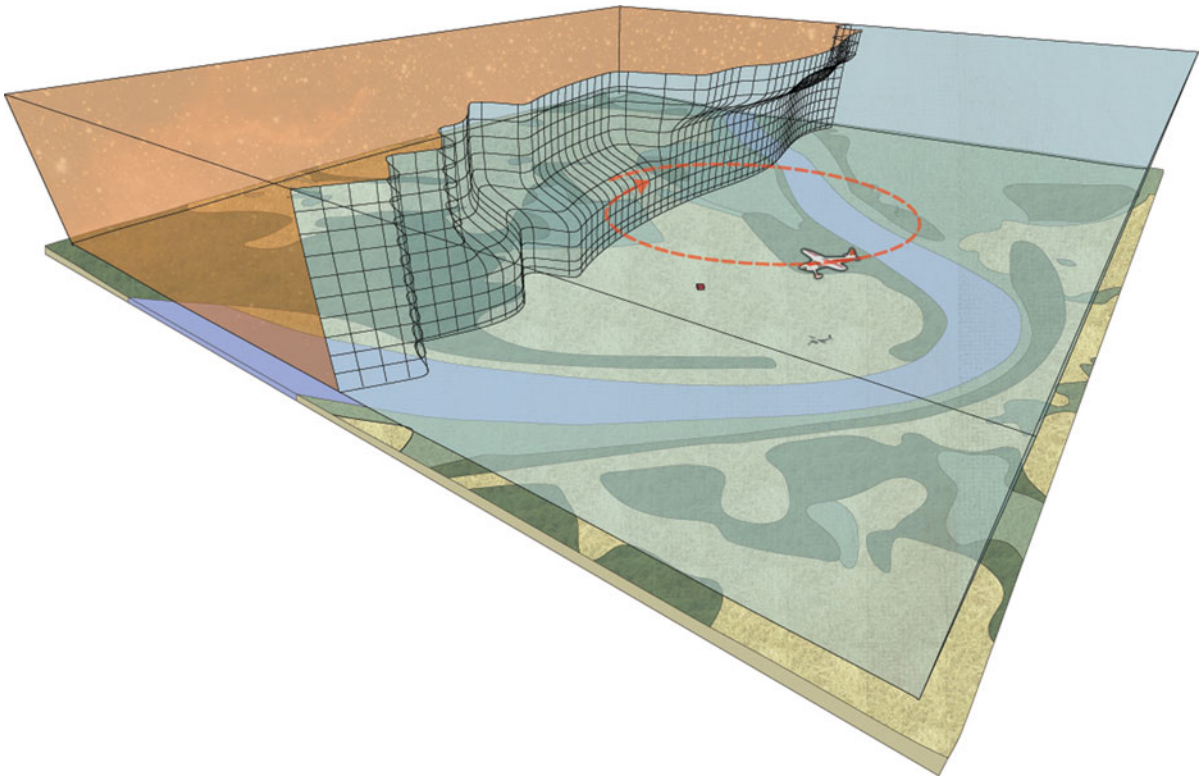

Fig. 2 Autonomous unmanned aerial vehicles (UAVs) are being used to collect *Fusarium* before and after a predicted atmospheric transport barrier (wire frame, exaggerated) passing over Virginia Tech's Kentland Farm in Blacksburg, VA

the NIV genotype, 14:00 UTC on May 1, 2007, to 16:00 UTC on May 1, 2007, with a 1 h spacing between reference times. The FTLE field and derived LCSs were computed from particle trajectories as in Lekien and Ross (2010). The LCS-based ATBs were found as one-dimensional curves that act as barriers to large-scale horizontal atmospheric transport. These curves are considered a horizontal slice (along the 900 hPa pressure surface) of essentially vertical two-dimensional ATB surfaces (see Fig. 2).

3 Results

3.1 Collections of *Fusarium*, species determination, and trichothecene genotypes

Fusarium graminearum was collected on 11 separate UAV flights 40–320 m AGL in 2006 and 2007 (Table 1). *F. graminearum* was just one of the species that was represented in our flight populations; 4–36 colonies of *Fusarium* were recovered from these flights (Table 1), and a detailed analysis of the additional species represented in these flight populations is the subject of ongoing work. Isolates I and J were collected during simultaneous sampling missions on the same day, with two UAVs flying at the same time but at different altitudes (Table 1). BLAST queries against Fusarium-ID and GenBank for TEF sequences from 10 isolates (A–G and I–K) showed 99–100% similarity to *F. graminearum* (high-quality TEF sequences from isolate H were not obtained). Microscopic observations of macroconidia were consistent with the morphology of *F. graminearum* as described by Leslie and Summerell (2006). *Tri3* and *Tri12* trichothecene genotypes were evaluated for all 11 isolates; 9 of the isolates were DON/15ADON, 1 isolate was DON/3ADON, and 1 isolate was NIV (Table 1).

3.2 Fusarium head blight and trichothecene mycotoxin production

All 11 isolates of *F. graminearum* produced symptoms of FHB on the spring wheat cultivar Norm

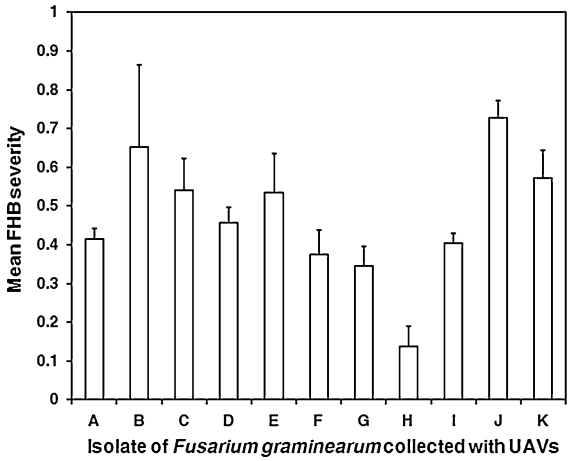

Fig. 3 All 11 isolates of *Fusarium graminearum* collected with autonomous unmanned aerial vehicles (*UAVs*) caused Fusarium head blight (*FHB*) on the spring wheat cultivar Norm under growth chamber conditions. Symptoms of *FHB* were observed 14 days following inoculation. Mean FHB severity (number of spikelets showing symptoms divided by the number of spikelets in a spike) is reported for three inoculated spikes for each isolate. *Error bars* represent the standard error of the mean

within 14 days following our inoculations (Fig. 3). None of the wounded, non-inoculated (control) plants produced symptoms of FHB. For the DON/3ADON isolate (K), FHB severity ranged from 0.4 to 0.7. For the nine DON/15ADON isolates, FHB severity ranged from 0.1 to 1.0. For the NIV isolate (G), FHB severity ranged from 0.3 to 0.4. At 14 days, the DON/15ADON and DON/3ADON isolates produced a range from $\leq$0.5 ppm to 259.7 ppm DON, and the NIV isolate produced an average of 2.0 ppm NIV. Levels of 3ADON and 15ADON were at or below our limit of detection at the final dilution that was sampled.

3.3 Modeling of ATBs

ATBs were computed at three consecutive times, separated by 3 h, and centered on the time of the collection of the NIV genotype, 15:00 UTC May 1, 2007. Figure 4 shows the ATBs at these times. The red (gray) curves represent repelling ATBs, and blue (dark gray) curves represent attracting ATBs. A circular cluster of air parcels spread over a 25 km radius centered on Kentland Farm and initialized at 15:00 UTC May 1, 2007 is used to represent the sampled air mass, shown in black in panels (d), (e), and (f). Notice that the sampled air mass is "sandwiched" between two repelling barriers that are roughly 50 km apart.

4 Discussion

The aerobiology of *Fusarium* is poorly understood. This is due, at least in part, to the lack of appropriate technologies for studying the aerobiology of these fungi. First, identification of *Fusarium* based solely on microscopic examination of a single spore from airborne samples (e.g., an Anderson spore sampler or a Rotorod sampler) is difficult due to the presence of other spores with similar morphologies. Identification beyond the level of genus requires culturing of representative spores, followed by careful examination of hyphae, conidiogenous cells, and different spore types (e.g., macroconidia, mesoconidia, microconidia, and chlamydospores) produced on standard culture media (Leslie and Summerell 2006). Traditional microscopic observations have more recently been accompanied by DNA sequence-assisted identification (Geiser et al. 2004), which is rapidly becoming the method of choice for accurate and robust identification of *Fusarium* to the level of species. Second, technologies for tracking the long-distance movement of *Fusarium* in the atmospheric boundary layer have been limited. Recently, Schmale and colleagues have developed, tested, and implemented new technologies with autonomous (self-controlling) unmanned aerial vehicles (UAVs) to study the movement of microorganisms such as *Fusarium* in the lower atmosphere (Schmale et al. 2008). Autonomous UAVs offer a number of advantages over platforms operated entirely by a ground-based pilot (e.g., Maldonado-Ramirez et al. 2005) including reducing pilot fatigue, maintaining precise sampling altitudes and sampling patterns, and coordinating the flight of multiple UAVs sampling at different altitudes (Techy et al. 2010).

DNA sequencing and morphological observations of macroconidia assisted in the identification of 11 isolates of *F. graminearum* collected from autonomous UAV flights conducted 40–320 m AGL during spring, summer, fall, and winter months. To our knowledge, this is the first report of the collection of *F. graminearum* in the atmospheric boundary layer during the fall and winter—two seasons that fall outside the normal growing season for small grains

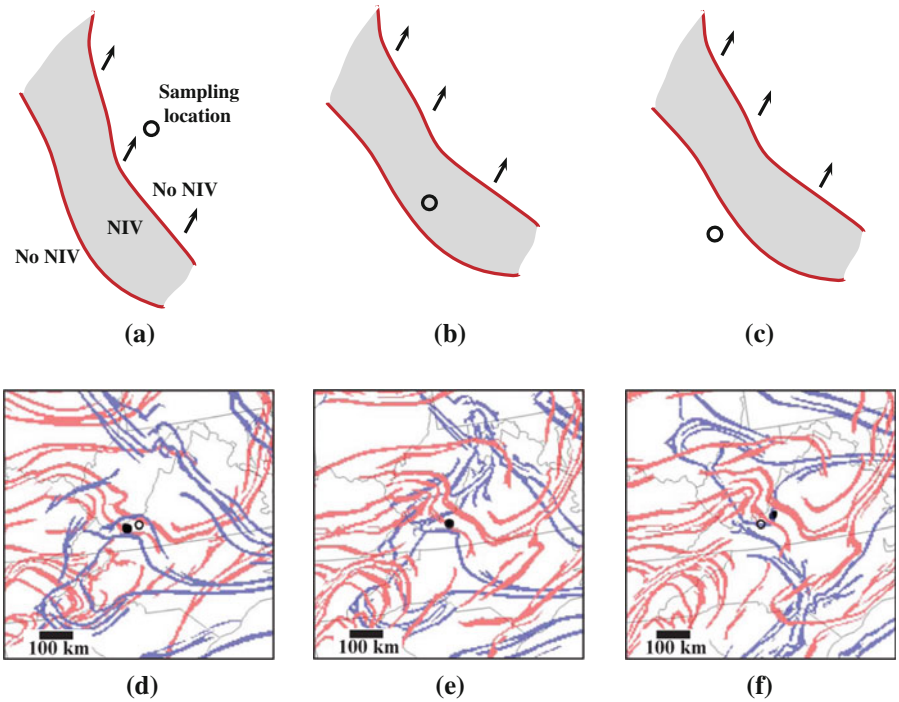

Fig. 4 Schematic showing the movement, with respect to a geographically fixed sampling location (*black circle*), of an air mass containing the NIV genotype of *F. graminearum.* The air mass is sandwiched between repelling atmospheric transport barriers (ATBs). As the air mass passes over the sampling location, the NIV genotype is sampled. Before and after the air mass passes over the sampling location, the NIV genotype is not detected. In the lower panel, we show the ATBs on the 900 hPa pressure surface computed from archived NOAA wind data, for the times surrounding the UAV flight which contained the NIV genotype (**a**)/(**d**) 12:00 UTC May 1, 2007, (**b**)/(**e**) 15:00 UTC May 1, 2007, and (**c**)/(**f**) 18:00 UTC May 1, 2007. The ATBs indicate the regions of highest separation between air parcel trajectories over ±24 h. *Red* (*gray*) *curves* indicate repelling ATBs (separation in forward time), and *blue* (*dark gray*) *curves* indicate attracting ATBs (separation in backward time). The *black air mass* in **d, e**, and **f** contained the NIV genotype and was sandwiched between two repelling ATBs. (*color in online version only*)

(e.g., spring wheat and barley) and corn in Virginia and neighboring states. The nearest growing regions that would support these crops during the fall and winter are likely to be in the southern part of the United States (e.g., Florida), many states away from Virginia. Previous work with UAVs in New York from 1999 to 2002 reported that viable spores of *F. graminearum* were ubiquitous in the atmosphere 60 meters AGL during May and June (time periods surrounding the flowering of local wheat) (Maldonado-Ramirez et al. 2005). Though the work by Maldonado-Ramirez et al. (2005) was among the first to provide a link between sources of *F. graminearum* in the atmospheric boundary layer and regional epidemics of FHB, the authors were unable to exclude local (on-farm) sources as potential contributors to their collections and thus were limited in their ability to speculate on realistic transport distances for the fungus. Our collections of *F. graminearum* during the fall and winter months were outside a reasonable sporulation and infection window for the fungus in Virginia (approximately April through August), providing a strong indication of long-distance transport of *F. graminearum* from regions outside of Virginia; it is unlikely that local inoculum sources at the Kentland Farm (or even in the state of Virginia) would have been operative during the cold fall and winter months. Thus, it seems reasonable to speculate that atmospheric transport distances for *F. graminearum* may be on the order of tens to hundreds of kilometers or more.

All 11 isolates of *F. graminearum* collected with UAVs produced symptoms of FHB on the spring

wheat cultivar Norm within 14 days following our inoculations (Fig. 3), and all of these isolates produced the trichothecene mycotoxins DON or NIV *in planta* consistent with their genotypes. Thus, the isolates of *F. graminearum* collected in the atmospheric boundary layer have the potential to be pathogens and toxin producers in real-world agricultural systems. This, of course, would ultimately depend on a suite of factors including (1) the ability of the spores to remain viable over the remainder of their journey through the atmosphere and (2) their arrival at a final destination with appropriate environmental conditions that would support infection.

Our collections of the NIV and DON/3ADON genotypes of *F. graminearum* in the atmospheric boundary layer were unexpected. Schmale et al. (2011) conducted a large survey of trichothecene genotypes of *F. graminearum* in 39 wheat fields in New York, Pennsylvania, Maryland, Virginia, Kentucky, and North Carolina in 2006. Ninety-two percent (919/998) of the isolates recovered from infected wheat spikes were DON/15ADON, 7% (69/998) were DON/3ADON, and 1% (10/998) was NIV. Isolates of the NIV genotype were only recovered in New York and North Carolina. To our knowledge, this is the first report of an isolate of *F. graminearum* of the NIV genotype in Virginia. In fact, 24-hour back trajectories of an air mass carrying the NIV genotype suggested an origin outside the state of Virginia. Moreover, though isolates of the DON/3ADON genotype were recovered in Virginia by Schmale et al. (2010), this genotype was rare in the populations of the fungus recovered from infected wheat plants, representing only about 2% (3/146) of the population studied in Virginia alone. The presence of novel mycotoxin producers (such as the NIV genotype of *F. graminearum*) in the atmospheric boundary layer has important implications for the movement of invasive genotypes (or even species) of *Fusarium* into previously unexposed regions. Our collections with UAVs yielded multiple colonies of *Fusarium* (Table 1) representing additional species, some of which are tentative pathogens and mycotoxin producers. Future work with UAVs and ground-level samplers aims to characterize the structure of these flight populations and ultimately link field and atmospheric collections of *Fusarium* at both local and regional scales.

The ATB framework developed here helps set the stage for new hypotheses concerning the origin, mixing, and long-distance transport of *Fusarium*. ATBs are moving boundaries between air masses; they are the regions of highest air parcel trajectory separation. Atmospheric populations of *Fusarium* moving passively are not expected to cross the evolving ATBs. ATBs can be large scale (hundreds of km in length), but with effects observed locally. For example, the air composition, in terms of trace chemicals and biota, on either side of an ATB is expected to be discontinuous. Therefore, ATBs are likely to be an important mechanism by which punctuated changes in the population structure of *Fusarium* can be understood, at fixed geographic locations and also at different locations at different times.

Recent observations by Gale et al. (2007), Guo et al. (2008), and Ward et al. (2008) suggest that field populations of *F. graminearum* in the Midwest and Canada are changing at an alarming rate. Populations of *F. graminearum* appear to be shifting from DON/15ADON genotypes to DON/3ADON genotypes, and the reason for this increase is still unknown. Ohe et al. (2010) inoculated wheat plots with multiple isolates of *F. graminearum* of both the DON/3ADON and DON/15ADON genotype. Significantly higher levels of DON were observed in two of the wheat lines studied, and these levels appeared to be associated with the DON/3ADON genotype. Perhaps, there are yet undiscovered fitness advantages associated with the DON/3ADON genotype that might confer rapid, local adaptation of the fungus in new regions. Such increased fitness might be coupled with punctuated episodes of long-distance transport of DON/3ADON (or even NIV) genotypes into new regions.

Acknowledgments We thank N. McMaster for her excellent technical assistance with the GC/MS. This material is based upon work supported by the National Science Foundation under Grant No. 0919088. Any opinions, findings, and conclusions or recommendations expressed in this material are those of the author(s) and do not necessarily reflect the views of the National Science Foundation.

References

Aylor, D. E. (2003). Spread of plant disease on a continental scale: Role of aerial dispersal of pathogens. *Ecology, 84*, 1989–1997.

Bowman, K. P., Pan, L. L., Campos, T., & Gao, R. (2007). Observations of fine-scale transport structure in the upper

troposphere from the High-performance Instrumented Airborne Platform for Environmental research. *Journal of Geophysical Research, 112*, D18111.

Bush, B. J., Carson, M. L., Cubeta, M. A., Hagler, W. M., & Payne, G. A. (2004). Infection and fumonisin production by *Fusarium verticillioides* in developing maize kernels. *Phytopathology, 94*, 88–93.

Chaimovitsh, D., Dudai, N., Putievsky, E., & Ashri, A. (2006). Inheritance of resistance to Fusarium wilt in sweet basil. *Plant Disease, 90*, 58–60.

d'Ovidio, F., Fernandez, V., Hernandez-Garca, E., & Lopez, C. (2004). Mixing structures in the Mediterranean Sea from finite-size Lyapunov exponents. *Geophysical Research Letters, 31*, L17203.

Dellnitz, M., Junge, O., Koon, W. S., Lekien, F., Lo, M. W., Marsden, J. E., et al. (2005). Transport in dynamical astronomy and multibody problems. *International Journal of Bifurcation and Chaos, 15*, 699–727.

Dill-Macky, R., & Jones, R. K. (2000). The effect of previous crop residues and tillage on Fusarium head blight of wheat. *Plant Disease, 84*, 71–76.

Dingus, B. R., Schmale, D. G., & Reinholtz, C. (2007). Development of an autonomous unmanned aerial vehicle for aerobiological sampling. *Phytopathology, 97*, S184.

Fernando, W. G. D., Miller, J. D., Seaman, W. L., Seifert, K., & Paulitz, T. A. (2000). Daily and seasonal dynamics of airborne spores of *Fusarium graminearum* and other *Fusarium* species sampled over wheat plots. *Canadian Journal of Botany, 78*, 497–505.

Francl, L., Shaner, G., Bergstrom, G., Gilbert, J., Pedersen, W., Dill-Macky, R., et al. (1999). Daily inoculum levels of *Gibberella zeae* on wheat spikes. *Plant Disease, 83*, 662–666.

Froyland, G., & Padberg, K. (2009). Almost-invariant sets and invariant manifolds—Connecting probabilistic and geometric descriptions of coherent structures in flows. *Physica D, 238*, 1507–1523.

Froyland, G., Padberg, K., England, M. H., & Treguier, A. M. (2007). Detection of coherent oceanic structures via transfer operators. *Physical Review Letters, 98*, 224503.

Gale, L. R., Ward, T. J., Balmas, V., & Kistler, H. C. (2007). Population subdivision of *Fusarium graminearum sensu stricto* in the upper midwestern United States. *Phytopathology, 97*, 1434–1439.

Geiser, D. M., Delmar Jimenez-Gasco, M., Kang, S., Makalowska, I., Veeraraghavan, N., Ward, T. J., et al. (2004). Fusarium-ID v.1.0: A DNA sequence database for identifying Fusarium. *European Journal of Plant Pathology, 110*, 473–479.

Goswami, R. S., & Kistler, H. C. (2005). Pathogenicity and in planta mycotoxin accumulation among members of the *Fusarium graminearum* species complex on wheat and rice. *Phytopathology, 95*, 1397–1404.

Guo, X. W., Fernando, W. G. D., & Seow-Brock, H. Y. (2008). Population structure, chemotype diversity, and potential chemotype shifting of *Fusarium graminearum* in wheat fields of Manitoba. *Plant Disease, 92*, 756–762.

Haller, G., & Yuan, G. (2000). Lagrangian coherent structures and mixing in two-dimensional turbulence. *Physica D, 147*, 352–370.

Ichinoe, M., Kurata, H., Sugiura, Y., & Ueno, Y. (1983). Chemotaxonomy of *Gibberella zeae* with special reference to production of trichothecenes and zearalenone. *Applied and Environmental Microbiology, 46*, 1364–1369.

Inanc, T., Shadden, S. C., & Marsden, J. E. (2005). Optimal trajectory generation in ocean flows. In *Proceedings of 2005 American Control Conference*, 674–679.

Isard, S. A., & Gage, S. H. (2001). *Flow of life in the atmosphere*. East Lansing: Michigan State University Press.

Katan, T., Shlevin, E., & Katan, J. (1997). Sporulation of *Fusarium oxysporum* f. sp. *lycopersici* on stem surfaces of tomato plants and aerial dissemination of inoculum. *Phytopathology, 87*, 712–719.

Lekien, F., Coulliette, C., Mariano, A. J., Ryan, E. H., Shay, L. K., Haller, G., et al. (2005). Pollution release tied to invariant manifolds: A case study for the coast of Florida. *Physica D, 210*, 1–20.

Lekien, F., & Ross, S. D. (2010). The computation of finite-time Lyapunov exponents on unstructured meshes and for non-Euclidean manifolds. *Chaos, 20*, 017505.

Leslie, J. F., & Summerell, B. A. (2006). *The fusarium laboratory manual* (p. 388). Ames, Iowa: Blackwell Publishing.

Maldonado-Ramirez, S. L., Schmale, D. G., Shields, E. J., & Bergstrom, G. C. (2005). The relative abundance of viable spores of *Gibberella zeae* in the planetary boundary layer suggests the role of long-distance transport in regional epidemics of Fusarium head blight. *Journal of Agricultural and Forest Meteorology, 132*, 20–27.

McMullen, M. P., Jones, R., & Gallenberg, D. (1997). Scab of wheat and barley: A re-emerging disease of devastating impact. *Plant Disease, 81*, 1340–1348.

Ohe, C., Gauthier, V., Tamburic-Ilincic, L., Brule-Babel, A., Fernando, W. G. D., Clear, R., et al. (2010). A comparison of aggressiveness and deoxynivalenol production between Canadian *Fusarium graminearum* isolates with 3-acetyl and 15-acetyldeoxynivalenol chemotypes in field-grown spring wheat. *European Journal of Plant Pathology, 127*, 407–417.

Reaver, D., & Schmale, D. G. (2007). High-throughput homogenization of grain samples for deoxynivalenol testing. Page 10 in Proc. 2007 National Fusarium Head Blight Forum, Kansas City, MO, December 2–4.

Schmale, D. G., Arntsen, Q. A., & Bergstrom, G. C. (2005). The forcible discharge distance of ascospores of *Gibberella zeae*. *Canadian Journal of Plant Pathology, 27*, 376–382.

Schmale, D.G., & Bergstrom, G.C. (2003). Fusarium head blight. *The Plant Health Instructor*. doi:10.1094/PHI-I-2003-0612-01.

Schmale, D. G., Dingus, B. R., & Reinholtz, C. F. (2008). Development and application of an autonomous unmanned aerial vehicle for precise aerobiological sampling above agricultural fields. *Journal of Field Robotics, 25*, 133–147.

Schmale, D. G., Fetters, T., Ross, S., Tallapragada, P., & Dingus, B. (2010). Isolates of *Fusarium graminearum* collected 40 to 300 meters above ground level cause *Fusarium* head blight and produce trichothecene mycotoxins. *Phytopathology, 100*, S208.

Schmale, D. G., & Gordon, T. R. (2003). Variation in susceptibility to pitch canker disease, caused by *Fusarium circinatum*, in native stands of *Pinus muricata*. *Plant Pathology, 52*, 720–725.

Schmale, D. G., Leslie, J. F., Saleh, A. A., Shields, E. J., & Bergstrom, G. C. (2006). Genetic structure of atmospheric populations of *Gibberella zeae*. *Phytopathology, 96*, 1021–1026.

Schmale, D.G., Wood-Jones, A.K., Cowger, C., Bergstrom, G.C., & Arellano, C. (2011). Trichothecene genotypes of *Gibberella zeae* from winter wheat fields in the eastern United States. *Plant Pathology*. doi:10.1111/j.1365-3059.2011.02443.x.

Senatore, C. & Ross, S. D. (2008). Fuel-efficient navigation in complex flows. In *Proceedings of 2008 American Control Conference*, 1244–1248.

Senatore, C. & Ross, S. D. (2011). Detection and characterization of transport barriers in complex flows via ridge extraction of the finite time Lyapunov exponent field. *International Journal for Numerical Methods in Engineering*. doi:10.1002/nme.3101.

Shadden, S. C., Lekien, F., & Marsden, J. E. (2005). Definition and properties of Lagrangian coherent structures: Mixing and transport in two-dimensional aperiodic flows. *Physica D, 212*, 271–304.

Shadden, S. C., & Taylor, C. A. (2008). Characterization of coherent structures in the cardiovascular system. *Annals of Biomedical Engineering, 36*, 1152–1162.

Stremler, M. A., Ross, S. D., Grover, P., & Kumar, P. (2011). Topological chaos and periodic braiding of almost-cyclic sets. *Physical Review Letters, 106*, 114101.

Tallapragada, P. (2010). *Identifying dynamical boundaries and phase space transport using Lagrangian coherent structures*. Ph.D. dissertation. Virginia Polytechnic Institute and State University, Blacksburg.

Techy, L., Schmale, D. G., & Woolsey, C. A. (2010). Coordinated aerobiological sampling of a plant pathogen in the lower atmosphere using two autonomous unmanned aerial vehicles. *Journal of Field Robotics, 27*, 335–343.

Tew Kai, E., Rossi, V., Sudre, J., Weimerskirch, H., Lopez, C., Hernandez-Garcia, E., et al. (2009). Top marine predators track Lagrangian coherent structures. *Proceedings of the National Academy of Sciences, 106*, 8245–8825.

Wang, B., & Jeffers, S. N. (2000). Fusarium root and crown rot: A disease of container-grown hostas. *Plant Disease, 84*, 980–988.

Ward, T. J., Bielawski, J. P., Kistler, H. C., Sullivan, E., & O'Donnell, K. (2002). Ancestral polymorphism and adaptive evolution in the trichothecene gene cluster of phytopathogenic *Fusarium*. *Proceedings of the National Academy of Sciences, 99*, 9278–9283.

Ward, T. J., Clear, R. M., Rooney, A. P., O'Donnell, K., Gaba, D., Patrick, S., et al. (2008). An adaptive evolutionary shift in Fusarium head blight pathogen populations is driving the rapid spread of more toxigenic *Fusarium graminearum* in North America. *Fungal Genetics and Biology, 45*, 473–484.